Marine Pollution Bulletin 153 (2020) 110948

Contents lists available at ScienceDirect

Marine Pollution Bulletin

journal homepage: www.elsevier.com/locate/marpolbul

Baseline

Measurements of underwater noise radiated by commercial ships at a cabled ocean observatory

Guosong Zhang[a,*], Tonje Nesse Forland[a], Espen Johnsen[a], Geir Pedersen[a], Hefeng Dong[b]

[a] Institute of Marine Research, Bergen, Norway
[b] Norwegian University of Science of Technology, Trondheim, Norway

ARTICLE INFO

Keywords:
Underwater noise
Sound pressure level
Ship passage
LoVe observatory
Automatic Identification System

ABSTRACT

Measurements of underwater noise radiated under ship normal operations are presented. The acoustic data, from the cabled ocean observatory, are analyzed under each identified ship passage, which was obtained by the Automatic Identification System. Under each passage, sound pressure level is calculated to observe local noise variations due to shipping noise. This paper emphasizes the study of noise variations at the observatory, presents the noise measurements under identified ship passages in the last several years, and provides references for predictive models of underwater noise pollution from commercial ship traffic. From the passages of one ship to the passages of 26 ships, the measurements reveal similar variation patterns when the ships traveled at similar courses, but different patterns when they traveled at different courses. When evaluating the noise variations due to ship traffics, it is important to consider the shipping noise propagation as well as ship movement.

Underwater noise radiated by ships is one of the main sources of anthropogenic components of the marine ambient noise (Hildebrand, 2009; McKenna et al., 2012; Wenz, 1962), and it becomes a significant source of noise pollution for the marine habitat, especially for those close to the ship traffic routes. E.g. cod are sensitive to low frequency tonal noise from 30 to 470 Hz (Chapman and Hawkins, 1973; Nordeide and Kjellsby, 1999), and marine mammals relying on sound as their primary sense can be concerned (Tyack, 2008). The long term observations show the ambient noise level at low frequencies increases with time (Andrew et al., 2002; McDonald et al., 2006), and it is primarily the result of increased commercial shipping activities. The shipping noise is generated under ship normal operations. When the local impact from the shipping noise are to be investigated, it is of importance to measure the noise in the field (McKenna et al., 2012), as sound propagation characteristics are also related to environmental conditions (Hovem, 2010).

The shipping noise is broadband noise, significantly at low frequencies of 50–150 Hz, and it can be up to 10 kHz (Ross, 1976). An ensemble model based on broadband measurements (Wales and Heitmeyer, 2002), up to 1200 Hz, where ship characteristics and movements are considered, and it is hard to be applied for a specific ship due to the noise source signature. The shipping noise up to 1 kHz frequencies were measured in April 2009 (McKenna et al., 2012), and the source levels of the categorized big ships (based on Lloyd Registry of Ships) are back calculated by the received sound pressure level (SPL) with the modeled transmission losses. Discussions between the calculated source level versus distance are shown, and they are only based on the starboard side measurements at the closest point of approach (CPA) of 3 km. In this study, the shipping noise was measured without preferences of the ship categories, and the local noise variations due to ship passages are of interests.

The acoustic data from 2014, 2015 and 2018 are used to study the shipping noise, which were recorded by a hydrophone close to the sea floor. The hydrophone was installed at the cabled ocean observatory, namely the LoVe observatory, which was deployed at Lofoten-Vesterålen, Nordland county, Norway (Fig. 1). The Lofoten area is a marine biological hot spot (Godø et al., 2014), e.g. it is one of the Arctic cod (*Gadus morhua* L.) spawning grounds (Nordeide and Kjellsby, 1999), the Lofoten islands also play a significant role for the costal marine ecology (Engeland et al., 2019), and it is of interests to measure the local noise variations because of the ship passages.

The LoVe observatory is currently operated by Institute of Marine Research (IMR), and it has been in operations since 2013 (Godø et al., 2014). It is a cabled observatory deployed at a water depth about 250 m, and it monitors long term oceanic dynamics. It has been a collaborative project between IMR, Equinor ASA, and Metas AS, and an extension is to be completed in 2020. The observatory consists of three subsea landers, one main lander and two satellite landers. There are

* Corresponding author.
E-mail address: guosong.zhang@hi.no (G. Zhang).

https://doi.org/10.1016/j.marpolbul.2020.110948
Received 3 October 2019; Received in revised form 24 January 2020; Accepted 28 January 2020

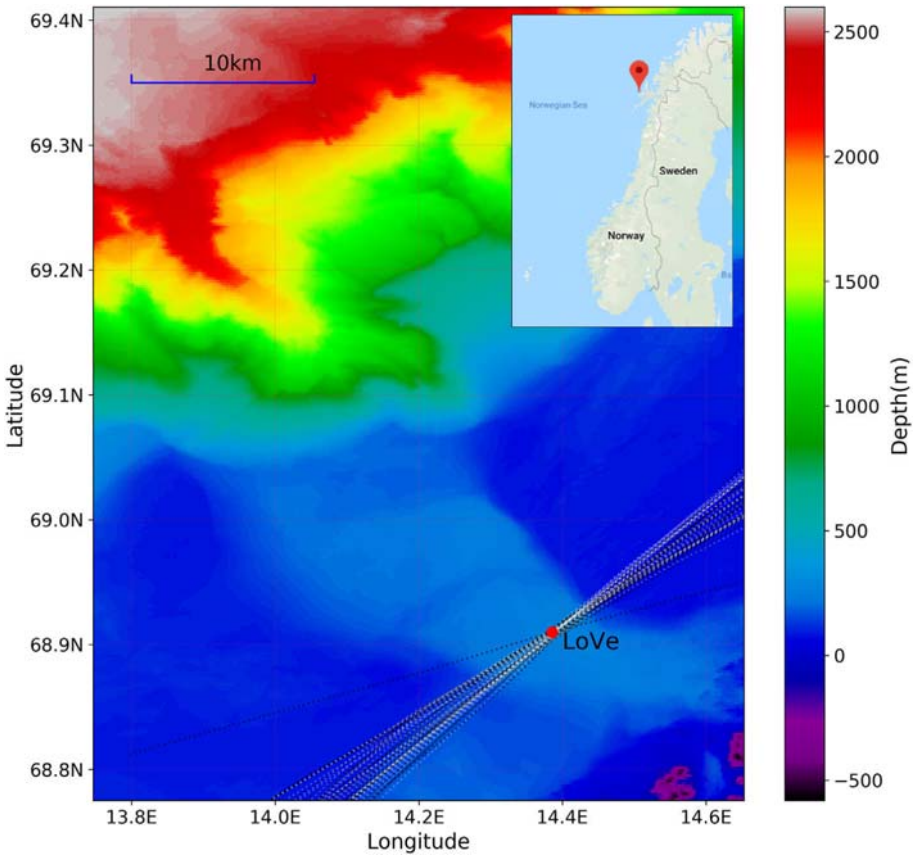

Fig. 1. Location of the LoVe observatory. The observatory was deployed close to cold water coral reefs, where the water depth is about 250 m. The dotted lines are selected ship passages in this paper. The black ones are the passages from North to South, and the white ones are from South to North. Bathymetry data are provided here courtesy of EMODnet (www.emodnet.eu).

different marine sensors installed on each lander, including acoustic Doppler current profilers, one broadband echo-sounder, one hydrophone and details of the infrastructure are given by Godø et al. (2014). Synchronized with Coordinated Universal Time (UTC), real time data from the observatory instruments are transferred to a station on shore, via fiber communications, and thereafter any users can access the historical data on the web portal https://love.equinor.com/.

The hydrophone (model icListen HF/SB35 ETH) made by Ocean Sonics was installed within one of the satellite landers, it is about 0.5 m above the seabed, and it has been continuously recording background noise while it is synchronized with UTC time, except when the observatory was under maintenance or outages of electricity. The hydrophone sampling rate is adjustable, e.g. a maximum rate of 512 kHz, and a 24-bit resolution to avoid amplitude clipping when ships come close to the observatory. The received sensitivity of the hydrophone was calibrated from 10 kHz to 200 kHz, in March 2017, where it varies within a range of 3 dB. In calculating SPL as follows, the received sensitivity -170 dB re 1 $V/\mu Pa$ is used.

Ships along the Norwegian coast are monitored by The Norwegian Costal Administration. Within 12 nautical miles along Norwegian coast, the ship tracking data from Automatic Identification System (AIS) can be downloaded at https://ais-public.kystverket.no/ais-download/. Each record of the AIS data includes a UTC time stamp, the International Maritime Organization (IMO) number that is the unique ship identifier during its life span, ship length, ship heading, and etc. The AIS data are used to select ship passages close to the observatory, when the passages are selected without noise interference from other ships that are also close to the observatory. Particularly, a radius of 20 km to the observatory is selected, and then one ship passage is only selected with the condition that there are no other ships within this area and during the time interval of this passage. In all, 54 passages of 26 ships were selected, and they have minimum surface distances less than 500 m to the observatory. During the passage selection, no post processing is applied to the AIS data.

The shipping noise is mostly below 2 kHz, and therefore the original data are decimated to a sampling frequency of 4 kHz. Under a selected ship passage, SPL is calculated to indicate the sound field variations at the observatory. Note that two general directions, namely South and North, are used to state the ship courses in movement. The passages are grouped into the two courses, namely from South to North and from North to South. Following the guide line (Robinson et al., 2014), the steps below describes how AIS is combined with SPL calculations.

1. SPL is calculated using the root mean square of sound pressure with a time interval of 1 s, without frequency weighting. SPL at recording time t is denoted as $SPL^T(t)$ that is calculated using the decimated acoustic data of 1 second time interval $[t, t+1]$.
2. Given by the position of the n_{th} AIS record, the distance d_n as slant range to the observatory is calculated, where the hydrophone depth is set as 250 m.
3. SPL at the distance d_n to the observatory, denoted as $SPL^D(d_n)$, is an averaged SPL of 10 s (linear scale), and it is calculated by $SPL^D(d_n) = mean[SPL^T({T_{AIS}}^n - 5), SPL^T({T_{AIS}}^n - 4), \ldots, SPL^T({T_{AIS}}^n + 4)]$, where ${T_{AIS}}^n$ is the timestamp of the n_{th} AIS record.

Fig. 2 shows the SPL variations under the ship Olympus passages, all of which have stable course over ground (COG) through the whole passages. COG from AIS is measured against the geographical north, particularly 0 degree, it shows the track relative to the seabed, and indicates the actual traffic route. Regardless of heading and other unknown factors, maximum SPL of each passage differentiates due to different CPAs, and the maximum SPL is about 140 dB re 1 μPa. The maximum SPL in Fig. 2(a) is similar to that in Fig. 2(b), and it indicates that the ship source level is almost the same in those years. SPL variations over the distance, before and after CPA, are significant different between Fig. 2(a) and (b). For the passages in Fig. 2(a), the stern aspect

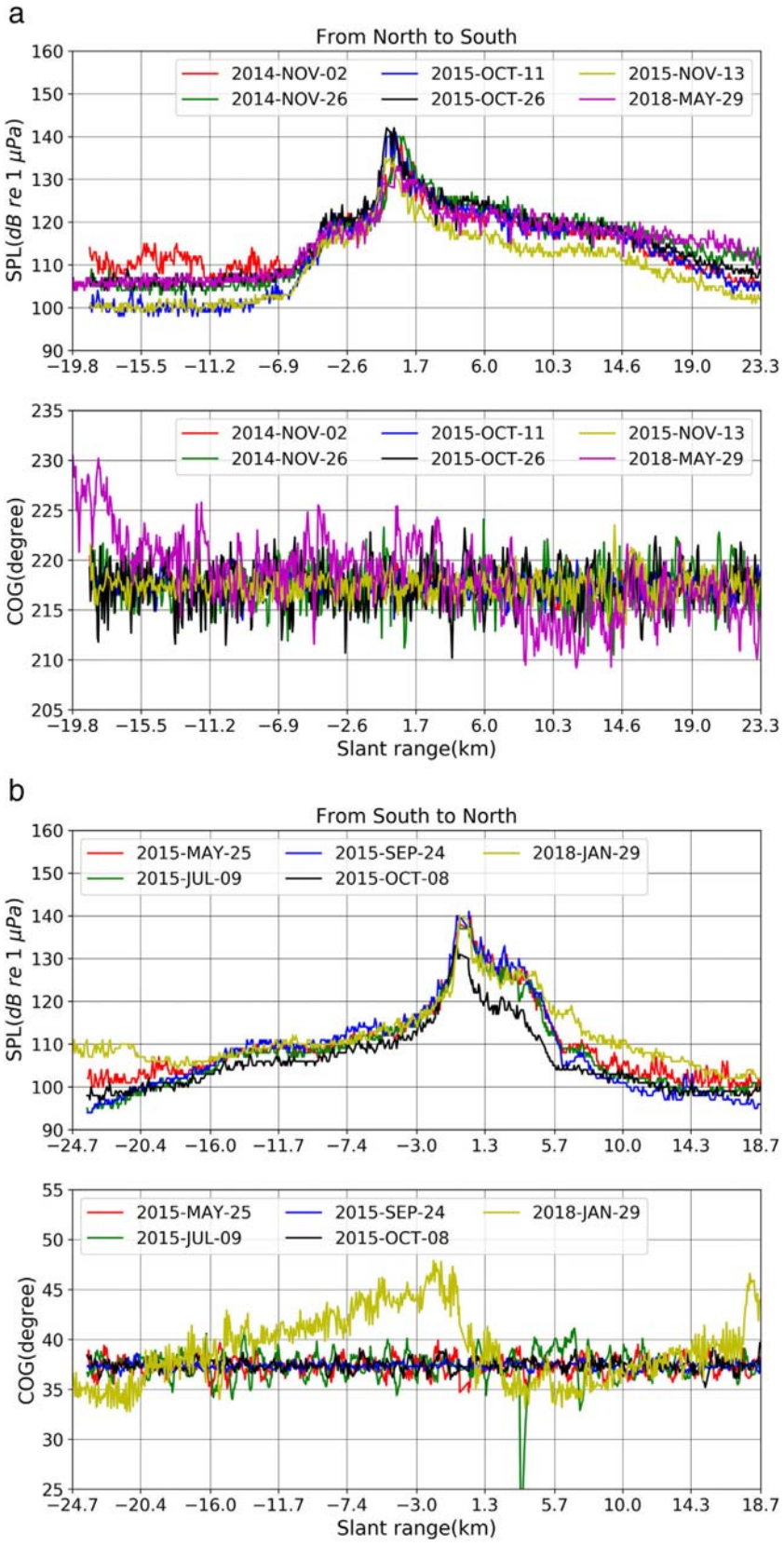

Fig. 2. SPL measurements under the passages of ship Olympus (IMO 9310355). Olympus is a chemical tanker of gross tonnage of 7515 tons. Negative slant range is approaching CPA and positive slant range is leaving CPA. (a) From North to South. (b) From South to North.

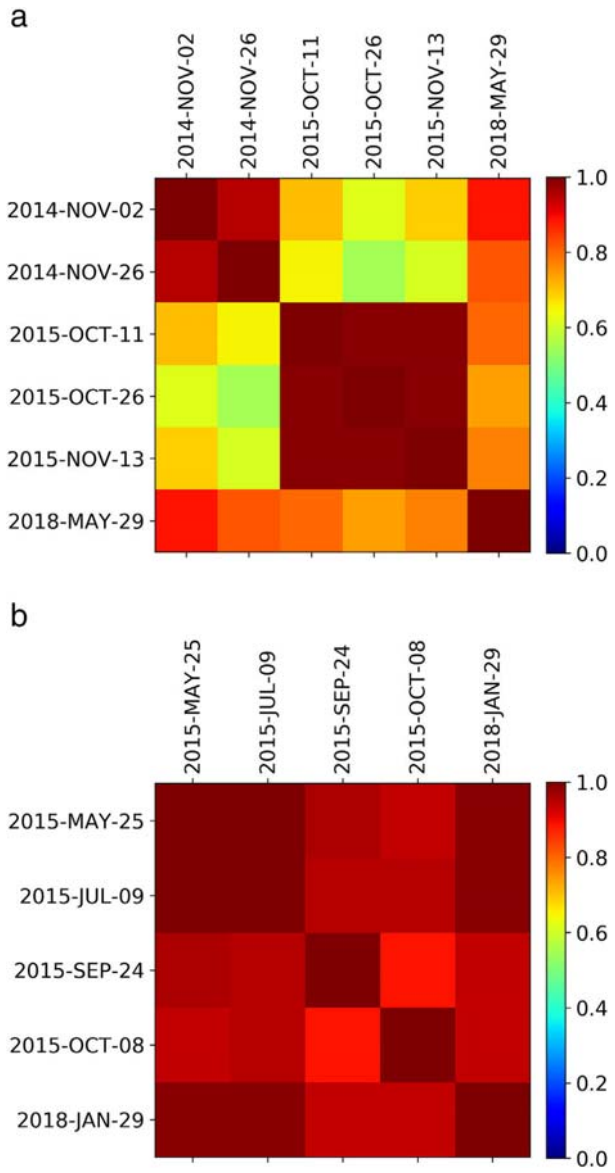

Fig. 3. Correlation coefficient matrix of SPL variations under the passages of Olympus (IMO 9310355). (a) From North to South, the minimum coefficient is 0.55. (b) From South to North, the minimum coefficient is 0.89.

SPL decreases by around 20 dB at a distance 15 km after CPA, while it decreases by around 20 dB at a distance of 5 km after CPA in Fig. 2(b). SPL also increases differently, when the ship approached the observatory from different directions.

SPL varies with the ship distance to the hydrophone, and the variation patterns are similar when the ship traveled in the same direction (Fig. 2). The pattern of each passage is described as a vector $[SPL^D(-18), SPL^D(-17), \ldots, SPL^D(18)]$ with a distance resolution of 1 km. Between one pair passages, the correlation coefficient (linear scale) is used to quantify the similarity. The correlation matrices in Fig. 3 show that there are high similarities for the passages of the same course, and the similarities are surprisingly higher among those from South to North in Fig. 3(b), in which the minimum correlation coefficient is 0.89 (between the passages of 2018-JAN-29 and 2015-OCT-08). The passages occurred in different time, and resulted in similar noise variations when Olympus traveled in the same direction.

54 passages in 2014, 2015 and 2018 have been selected, and SPL measurements of the passages are presented in Fig. 4. Given by COG, it is seen that the passages hade stable and similar courses when they traveled in the same direction. In Fig. 4(a), before CPA, the standard deviations (the black circles) of SPL measurements are larger at large distances, and it reduces to the smallest at a distance of 6 km. In Fig. 4(b), the standard deviation is surprisingly small before CPA, which indicates that those different ships at those distances had similar SPL variations at the observatory, and it increases after CPA. Comparing Fig. 4(a) with Fig. 4(b), before CPA, the standard deviations are obviously smaller in Fig. 4(b), and this observation correlates well with the quantifications in Fig. 3 in which the variation patterns are most similar for the passages from South to North. Although it is well known that the ships have different noise characteristic (Arveson and Vendittis, 2000; Trevorrowa and Vasiliev, 2008), it is interesting to observe the higher similarities in Fig. 4(b) and the lower similarities in Fig. 4(a).

Bow aspect shipping noise measurements are taken before CPA, and stern aspect measurements are taken after CPA (McKenna et al., 2012). On observing the mean SPL values at a distance of 15 km, the stern aspect SPL is 7.2 dB higher than the bow aspect SPL in Fig. 4(a); the bow aspect SPL is 3.4 dB higher than the stern aspect SPL in Fig. 4(b). Depending on the travel directions, the bow aspect noise could result in higher impact at the observatory at large distances, although the stern aspect noise levels are 5 to 10 dB higher than the bow aspect noise levels (McKenna et al., 2012). In addition, the SPL increases and decreases differently between Fig. 4(a) and (b), when the ships approached and left the observatory. Although the directivity of the ship source noise can be neglected at large distances, e.g. 15 km, it does not apply that the measurements are symmetrical. For the ship Olympus, $SPL^D(15)$ in Fig. 2(a) is about 10 dB larger than $SPL^D(-15)$ in Fig. 2(b).

This study presents measurements of underwater radiated noise by commercial vessels which traveled nearby the LoVe observatory. Combined with AIS, the noise level as SPL at the observatory is calculated during the identified ship passages. For the 11 passages of the single ship Olympus, it is revealed that there are similar noise variations at the observatory when it traveled at similar courses, when the passages occurred at different time of the years. For the 54 passages of 26 ships, the SPL varied more similar when the ships approached CPA from South to North, and varied quite differently when the ships traveled towards different directions. It can be concluded that the local noise variations are also determined by the shipping noise propagation, and let alone different noise source characteristics. Therefore, when the shipping noise impact is to be evaluated, it is recommended to consider the noise propagation, given by the local sound propagation conditions, as well as the ship tracking information given by AIS.

There are some uncertainties and challenges in the measurements. Firstly, the hydrophone was not calibrated at low frequencies less than 10 kHz, and therefore each SPL value has uncertainty. On evaluating the shipping noise impact, it is also important to study the SPL variations against the ship movements as shown above, when the calibration is a minor issue here.

For the passages identified by AIS, noise interference from other ships might happen. According to the Norwegian Costal Administration, the ships less than 45 m are not required to have AIS. In practice, some ships might turn off the AIS. Besides, the ship load, oceanographic, speed through water, weather conditions of the passages and etc. are unknown, and they could be quite different during those measurements. The ship noise source level can be different at different speed through water, and a stormy weather could result in higher ambient noise level (Wenz, 1962). However, the AIS data are the best available ship traffic data to be combined with the acoustic data.

The ship acoustic signature, including spatial directivity, is unknown. In some passages, it is observed that the maximum SPL did not occur at CPA, although only the passages of surface distances less than 500 m were selected in this paper. Since data from the LoVe observatory are time synchronized with AIS, it is most probably due to the ship spatial characteristics. On measuring the SPL at a distance in terms of several kilometers, the problem that the maximum SPL does not

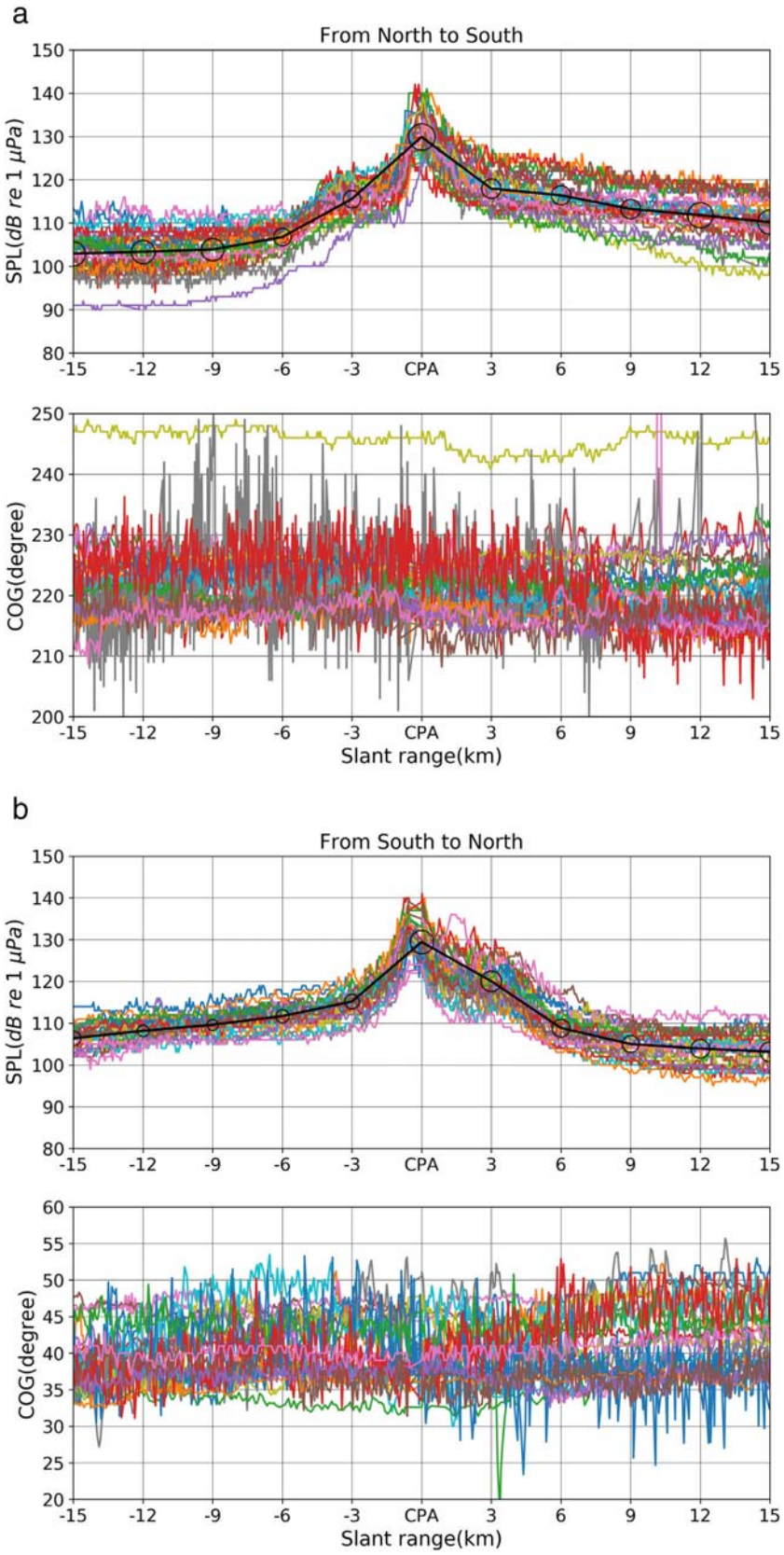

Fig. 4. SPL measurements of 54 passages of 26 ships in 2014, 2015, and 2018. Negative slant range is approaching CPA and positive slant range is leaving CPA. (a) From North to South. (b) From South to North. In each upper panel, the solid black line with circles shows mean values at those distances, where the size of a circle shows the scale of standard deviation, and both (a) and (b) use the same scale.

occur at CPA is thought minor in this study. The spatial characteristics could be better understood when other hydrophones will be fully integrated to the LoVe observatory in 2020.

CRediT authorship contribution statement

Guosong Zhang: Investigation, Data curation, Writing - original draft, Writing - review & editing. **Tonje Nesse Forland:** Writing - review & editing. **Espen Johnsen:** Funding acquisition, Writing - review & editing. **Geir Pedersen:** Writing - review & editing. **Hefeng Dong:** Writing - review & editing.

Declaration of competing interest

No conflict of interest exists.

Acknowledgement

The authors special thank Harald Åsheim and Ola Brandt from Norwegian Coastal Administration, who assisted in obtaining AIS data. We also thank support from Equinor ASA, Norway, and the Research Council of Norway for funding the Lofoten-Vesterålen cabled observatory.

References

Andrew, R.K., Howe, B.M., Mercer, J.A., Dzieciuch, M.A., 2002. Ocean ambient sound: comparing the 1960s with the 1990s for a receiver off the California coast. Acoust. Res. Lett. Online 3, 65–70.
Arveson, P.T., Vendittis, D.J., 2000. Radiated noise characteristics of a modern cargo ship. J. Acoust. Soc. Am. 107, 118–129.
Chapman, C.J., Hawkins, A.D., 1973. A field study of hearing in the cod, Gadus morhua L. J. Comp. Physiol. 85, 147–167.
Engeland, T.V., Godø, O.R., Johnsen, E., Duineveld, G.C.A., Oevelen, D., 2019. Cabled ocean observatory data reveal food supply mechanisms to a cold-water coral reef. Prog. Oceanogr. 172, 51–64.
Godø, O.R., Johnsen, S., Torkelsen, T., 2014. The LoVe ocean observatory is in operation. Mar. Technol. Soc. J. 48, 24–30.
Hildebrand, J.A., 2009. Anthropogenic and natural sources of ambient noise in the ocean. Mar. Ecol. Prog. Ser. 395, 5–20.
Hovem, J.M., 2010. Marine Acoustics: The Physics of Sound in Underwater Environments. Peninsula Publishing.
McDonald, M.A., Hildebrand, J.A., Wiggins, S.M., 2006. Increases in deep ocean ambient noise in the Northeast Pacific west of San Nicolas Island, California. J. Acoust. Soc. Am. 120, 711–718.
McKenna, M.F., Ross, D., Wiggins, S.M., Hildebrand, J.A., 2012. Underwater radiated noise from modern commercial ships. J. Acoust. Soc. Am. 131, 92–103.
Nordeide, J.T., Kjellsby, E., 1999. Sound from spawning cod at their spawning grounds. ICES J. Mar. Sci. 56, 326–332.
Robinson, S., Lepper, P., Hazelwood, R.A., 2014. Good Practice Guide for Underwater Noise Measurement.
Ross, D., 1976. Mechanics of Underwater Noise. Pergamon, New York.
Trevorrowa, M.V., Vasiliev, B., 2008. Directionality and maneuvering effects on a surface ship underwater acoustic signature. J. Acoust. Soc. Am. 124, 767–778.
Tyack, P.L., 2008. Implications for marine mammals of large-scale changes in the marine acoustic environment. J. Mammal. 89, 549–558.
Wales, S.C., Heitmeyer, R.M., 2002. An ensemble source spectra model for merchant ship-radiated noise. J. Acoust. Soc. Am. 111, 1211–1231.
Wenz, G.M., 1962. Acoustic ambient noise in the ocean: spectra and sources. J. Acoust. Soc. Am. 34, 1936–1956.